# Novel Backbone Conformation of Cyclosporin A: The Complex with Lithium Chloride

**Matthias Köck,[†] Horst Kessler,*,[†] Dieter Seebach,[‡] and Adrian Thaler[‡]**

*Contribution from the Organisch-Chemisches Institut, Technische Universität München, Lichtenbergstrasse 4, D-8046 Garching, Germany, and Laboratorium für Organische Chemie der Eidgenössischen Technischen Hochschule, ETH Zentrum, Universitätstrasse 16, CH-8092 Zürich, Switzerland. Received October 21, 1991*

**Abstract:** The complexation of cyclosporin A (CsA) with lithium chloride (LiCl) in THF-$d_8$ has been examined by NMR at different concentrations of LiCl. With 3 equiv of LiCl both forms of CsA, complexed and uncomplexed, are visible while at higher concentrations of lithium chloride only one conformation is observed. Two-dimensional NMR methods were used to assign the $^1$H and $^{13}$C NMR spectra of cyclosporin A in THF-$d_8$ with and without addition of excess LiCl (30.9 equiv). For the lithium-complexed CsA (Li·CsA) NOE buildup rates were measured at five mixing times at 600 MHz. The conformation has been determined by restrained molecular dynamics calculations in vacuo and an iterative relaxation matrix approach to take spin-diffusion effects into account. The lithium-complexed CsA adopts a conformation completely different from the uncomplexed CsA in THF-$d_8$. The latter is almost identical to the known conformation of CsA in CDCl$_3$. The configuration of the peptide bond between MeLeu$^9$ and MeLeu$^{10}$ in the lithium complex has changed from cis to trans and all transannular hydrogen bonds are disrupted in the complex, similar in this regard to the recently published conformation of CsA bound to its natural receptor cyclophilin (CyP) even though differences in the backbone conformation exist. The conformations of CsA in CDCl$_3$, complexed to LiCl in THF, and bound to the receptor (CsA·CyP) in H$_2$O are compared and discussed in light of the biological activity of this important drug.

## Introduction

Cyclosporin A,[1] *cyclo*(-MeBmt$^1$-Abu$^2$-Sar$^3$-MeLeu$^4$-Val$^5$-MeLeu$^6$-Ala$^7$-D-Ala$^8$-MeLeu$^9$-MeLeu$^{10}$-MeVal$^{11}$-) (CsA, Figure 1), is an important drug widely used clinically to prevent graft rejection in bone marrow and organ transplantations. The immunosuppressive activity of CsA is related to the inhibition of the T-cell activation. Many different synthetic and natural cyclosporins have been tested, but CsA is still the most active.[2] The exact biological mechanism is unknown,[3] but the immunosuppressive activity of CsA may be linked to its affinity for the protein cyclophilin (CyP).[4] The X-ray and NMR structure of CyP was recently published.[5] The binding of CsA to cyclophilin has been correlated with the immunosuppressive activity.[6] An exception to this correlation is MeAla$^6$-CsA, which showed a significant degree of binding to CyP but only very weak immunosuppressive activity.[6,7] It was shown that cyclophilin has the same amino acid sequence as peptidyl prolyl cis/trans isomerase (PPIase), an enzyme that catalyzes the cis/trans isomerization of Xaa–Pro peptide bonds.[8] Cyclosporin A is a potent inhibitor of this enzyme, suggesting that some of the biological effects of CsA are correlated to the blocking of the enzyme activity of cyclophilin. An alternative has been suggested, CsA·CyP itself is the active species which interacts with another target.[9] Recently another immunosuppressive compound with higher biological activity, FK506, was discovered.[10] It does not bind to cyclophilin, but binds tightly to a second class of PPIases, FKBP.[11]

Cyclosporin A in CDCl$_3$ has been the subject of several NMR investigations,[12] the data used to examine different approaches to determine the conformation.[13] CsA contains only lipophilic amino acids, seven of which are N-methylated (position 1, 3, 4, 6, 9, 10, and 11). The N-methylation gives rise to the possibility of the occurrence of cis/trans isomers about the peptide bond, interconverting slowly on the NMR time scale. The barrier of cis/trans isomerization is ~75 kJ/mol for a normal peptide bond.[14] In addition, N-methylation leads to a drastic reduction of the $\phi$, $\psi$ conformational space.[15]

Due to its lipophilic character, the solubility of CsA in water is too low for a quantitative conformational analysis to be carried out.[16] In polar solutions, such as DMSO-$d_6$, several conformations in equilibrium slow on the NMR time scale are observed.[12a] Studies of CsA in THF-$d_8$, indicate one dominant conforma-

tion,[17,18] as found in CDCl$_3$ and C$_6$D$_6$.[12a] In CDCl$_3$ a second conformation is populated by 6% and shows a cis configuration

(1) (a) Rüegger, A.; Kuhn, M.; Lichti, H.; Loosli, H.-R.; Huguenin, R.; Quiquerez, C.; von Wartburg, A. *Helv. Chim. Acta* 1976, *59*, 1075-1092. (b) Borel, J. F.; Feurer, C.; Gubler, H. U.; Stähelin, H. *Agents Actions* 1976, *6*, 468-475. (c) Dreyfuss, M.; Härri, E.; Hofmann, H.; Kobel, H.; Pache, W.; Tscherter, H. *Eur. J. Appl. Microbiol.* 1976, *3*, 125-133. (d) Petcher, T. J.; Weber, H.-P.; Rüegger, A. *Helv. Chim. Acta* 1976, *59*, 1480-1488.

(2) For example, see: (a) Wenger, R. M. *Angew. Chem., Int. Ed. Engl.* 1985, *24*, 77-85. (b) Wenger, R. M. In *Progress in Allergy*; Kallos, P., et al., Eds.; S. Karger: Basel, 1986; pp 46-64. (c) Traber, R.; Hofmann, H.; Loosli, H.-R.; Ponelle, M.; von Wartburg, A. *Helv. Chim. Acta* 1987, *70*, 13-36. (d) Lee, J. P.; Dunlap, B.; Rich, D. H. *Int. J. Pept. Protein Res.* 1990, *35*, 481-494.

(3) For a review of the immunosuppressive mechanism, see: Schreiber, S. L. *Science* 1991, *251*, 283-287.

(4) Handschuhmacher, R. E.; Harding, M. W.; Rice, J.; Drugge, R. J.; Speicher, D. W. *Science* 1984, *226*, 544-547.

(5) (a) Kallen, J.; Spitzfaden, C.; Zurini, M. G. M.; Wider, G.; Widmer, H.; Wüthrich, K.; Walkinshaw, M. D. *Nature* 1991, *353*, 276-279. (b) Wüthrich, K.; Spitzfaden, C.; Memmert, K.; Widmer, H.; Wider, G. *FEBS Lett.* 1991, *285*, 237-247.

(6) Durette, P. L.; Boger, J.; Dumont, F.; Firestone, R.; Frankshun, R. A.; Koprak, S. L.; Lin, C. S.; Melino, M. R.; Pessolano, A. A.; Pisano, J.; Schmidt, J. A.; Sigal, N. H.; Staruch, M. J.; Witzel, B. E. *Transplant Proc.* 1988, *20*, 51-57.

(7) Gooley, P. R.; Durette, P. L.; Boger, J.; Armitage, I. M. *Int. J. Pept. Protein Res.* 1991, *37*, 351-363.

(8) (a) Takahashi, N.; Hayano, T.; Suzuki, M. *Nature* 1989, *337*, 473-475. (b) Fischer, G.; Wittmann-Liebold, B.; Lang, K.; Kiefhaber, T.; Schmid, F. X. *Nature* 1989, *337*, 476-478.

(9) (a) Friedman, J.; Weissman, I. *Cell* 1991, *66*, 799-806. (b) Liu, J.; Farmer, D., Jr.; Lane, W. S.; Friedman, J.; Weissman, I.; Schreiber, S. L. *Cell* 1991, *66*, 807-815.

(10) (a) Tanaka, H.; Kuroda, A.; Marusawa, H.; Hatanka, H.; Kino, T.; Goto, T.; Hashimoto, M.; Taga, T. *J. Am. Chem. Soc.* 1987, *109*, 5031-5033. (b) Thomson, A. W. *Immunol. Today* 1989, *10*, 6-9.

(11) (a) Sierkierka, J. J.; Hung, S. H. Y.; Poe, M.; Lin, C. S.; Sigal, C. S. *Nature* 1989, *341*, 755-757. (b) Harding, M. W.; Galat, A.; Uehling, D. E.; Schreiber, S. L. *Nature* 1989, *341*, 758-760. (c) Moore, J. M.; Peattie, D. A.; Fitzgibbon, M. J.; Thomson, J. A. *Nature* 1991, *351*, 248-250. (d) Mishnick, J. A.; Rosen, M. K.; Wandless, T. J.; Karplus, M.; Schreiber, S. L. *Science* 1991, *252*, 836-839.

(12) (a) Kessler, H.; Loosli, H.-R.; Oschkinat, H. *Helv. Chim. Acta* 1985, *68*, 661-681. (b) Loosli, H.-R.; Kessler, H.; Oschkinat, H.; Weber, H.-P.; Petcher, T. J.; Widmer, A. *Helv. Chim. Acta* 1985, *68*, 682-704. (c) Kessler, H.; Köck, M.; Wein, T.; Gehrke, M. *Helv. Chim. Acta* 1990, *72*, 1818-1832.

(13) (a) Lautz, J.; Kessler, H.; Kaptein, R.; van Gunsteren, W. F. *J. Comput.-Aided Mol. Des.* 1987, *1*, 219-241. (b) Lautz, J.; Kessler, H.; Blaney, J. M.; Scheek, R. M.; van Gunsteren, W. F. *Int. J. Pept. Protein Res.* 1989, *33*, 281-288. (c) Lautz, J.; Kessler, H.; Weber, H.-P.; Wenger, R. M.; van Gunsteren, W. F. *Biopolymers* 1990, *29*, 1669-1687. (d) Beusen, D. D.; Iijima, H.; Marshall, G. R. *Biochem. Pharmacol.* 1990, *40*, 173-175. (e) Pachter, R.; Altman, R. B.; Czaplicki, J.; Jardetzky, O. *J. Magn. Reson.* 1991, *92*, 468-479.

* Address correspondance to this author.
† Technische Universität München.
‡ ETH Zürich.

*Novel Backbone Conformation of Cyclosporin A*

*J. Am. Chem. Soc., Vol. 114, No. 7, 1992* 2677

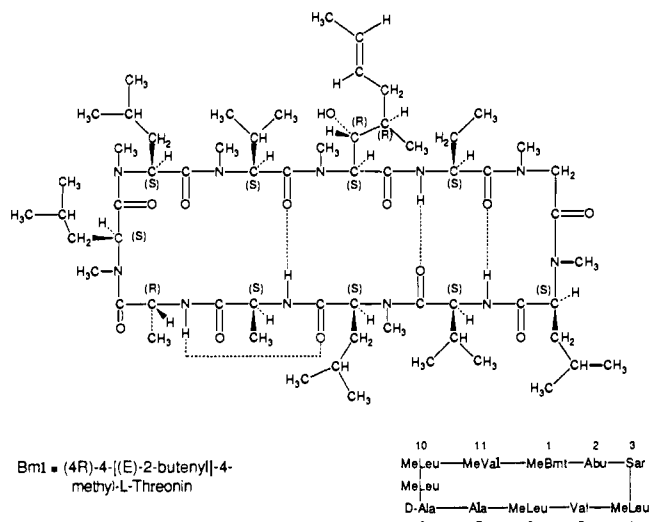Bml = (4R)-4-[(E)-2-butenyl]-4-methyl-L-Threonin

**Figure 1.** Constitution and residue numbering of cyclosporin A (CsA, molecular weight 1202.6).

of the peptide bond between the residues Sar[3] and MeLeu[4] in addition to the common one between MeLeu[9] and MeLeu[10].[19] Recently it was shown, that in [(C=S)MeBmt][1]-CsA (where an oxo amide is substituted by a thioamide in position 1) the population of the isomer with two cis peptide bonds is increased to 42%.[20]

Recent investigations of [13]C- and ^{15}N-enriched substrates using multidimensional X-filtered or X-half-filtered NMR techniques[21] allowed the determination of the conformation of CsA while bound to the natural receptor cyclophilin.[22] The surprise in these studies was that CsA when bound to CyP adopts a conformation which is completely different from the one found in solvents of low polarity or in the crystal. Hence, there is now clear evidence that the conformation of CsA is changed when going from solution to the receptor-bound state. A similar observation was made for FK506.[23] In view of these facts, it is of great interest to study CsA in different media in order to determine its flexibility and the occurrence of additional conformations.

## Complexation of CsA by Lithium Salts

The solvent tetrahydrofuran with addition of lithium salts has been shown to have a great effect on the solubility of peptides.[24] The essentially insoluble (<2 mg·mL⁻¹) Boc-Ala-Gly-Gly-Gly-OH could be solubilized to the extend of >300 mg·mL⁻¹ in this solvent by addition of 6 equiv of LiCl. It was evident from NMR studies, for instance of Boc-Gly-Gly-Nva-OH, that the peptides undergo conformational changes with the addition of LiCl, which led to

the proposal that unusual conformations of peptides could be studied in THF-$d_8$/LiCl solutions[24] (vide infra). The complexation was also used to disrupt inter-peptide aggregations and thus improve solubility and solid-phase peptide synthesis of certain fragments.[25] The formation of complexes between lithium salts and peptides, as well as the influence of salts on the solubility of amino acids and peptides, was first recognized by Pfeiffer at the beginning of the century.[26] Pfeiffer found, for instance, that small peptides can be precipitated from aqueous solution by addition of alkali halides. Some crystal structures of peptide·LiX complexes have been published.[27] In addition, NMR investigations of a cyclic pentapeptide and its dimer with LiClO₄ have appeared.[28]

Cyclosporin A has a solubility in THF at room temperature of more than 600 mg·mL⁻¹ and more than 300 mg·mL⁻¹ at −75 °C.[17,29] CsA may be considered as a solubilizing reagent for LiCl in THF: a LiCl concentration of up to 65 mg·mL⁻¹ can be obtained with CsA compared to 48 mg·mL⁻¹ without CsA. Lithium salts containing solutions of CsA[29] or of other peptides,[29,30] or phosphono peptides,[31] can be used for generating polylithiated derivatives such as hexalithio-CsA with BuLi or lithium diisopropylamide (LDA). Depending upon the type and amount of LiX [LiCl, LiBr, LiN(CHMe₂)₂] added, CsA can thus be alkylated on the CH₂ group of Sar[3], with formation of either an (R) or (S) stereogenic center.[29] These data illustrate the dramatic effect of the lithium salt on the conformation of the intermediates involved.

Rich et al. have used LiCl in THF or TFE as an improved solvent system for the determination of the PPIase activity.[32] The addition of the lithium salt leads to an increase of the population of cis Xaa-Pro isomers in some peptides. They have shown that the cis MeLeu[9]-MeLeu[10] CsA isomer is completely inactive as a PPIase inhibitor on a few minute time scale, whereas the trans isomer (CsA + LiCl in THF) is a tight-binding PPIase inhibitor.[33]

Here we report the conformation of CsA in THF-$d_8$ with a large excess of LiCl (see Figure 2).[17,34] This conformation is of special interest, because preliminary studies provided evidence that all peptide bonds are trans,[35] as found in the complex of CsA with cyclophilin (CsA·CyP). Therefore, no rotation about a peptide bond, which normally requires high activation energy, is necessary for binding to CyP. We will, however, show that the structure on complexation with LiCl is different from the one in the cyclophilin complex.

## NMR Measurements

**Resonance Assignment.** A detailed study using several homo- and heteronuclear 2D NMR techniques[36] was carried out to assign

(14) (a) Kessler, H. *Angew. Chem., Int. Ed. Engl.* **1970**, *9*, 219–235. (b) Stewart, W. E.; Siddall, T. H. *Chem. Rev.* **1970**, *70*, 517–551.

(15) Srinivasan, A. R.; Ponnuswamy, P. K. *Polymer* **1977**, *18*, 107–110.

(16) Hsu, V. L.; Heald, S. L.; Harding, M. W.; Handschuhmacher, R. E.; Armitage, I. M. *Biochem. Pharmacol.* **1990**, *40*, 131–140.

(17) Thaler, A. Dissertation No. 9454, ETH Zürich, 1991.

(18) Kessler, H.; Gehrke, M.; Lautz, J.; Köck, M.; Seebach, D.; Thaler, A. *Biochem. Pharmacol.* **1990**, *40*, 169–173, erratum 2185–2186.

(19) Widmer, H., Sandoz Pharma AG, Basel, personal communication. There exists no complete structure of this conformer.

(20) Seebach, D.; Ko, S. Y.; Kessler, H.; Köck, M.; Reggelin, M.; Schmieder, P.; Walkinshaw, M. D.; Bölsterli, J. J.; Bevec, D. *Helv. Chim. Acta* **1991**, *74*, 1953–1990.

(21) Otting, G.; Wüthrich, K. *Q. Rev. Biophys.* **1990**, *23*, 39–96.

(22) (a) Fesik, S. W.; Gampe, R. T., Jr.; Holzman, T. F.; Egan, D. A.; Edalji, R.; Luly, J. R.; Simmer, R.; Helfrich, R.; Kishore, V.; Rich, D. H. *Science* **1990**, *250*, 1406–1409. (b) Weber, C.; Wider, B.; von Freyberg, B.; Traber, R.; Braun, W.; Widmer, H.; Wüthrich, K. *Biochemistry* **1991**, *30*, 6563–6574. (c) Fesik, S. W.; Gampe, R. T., Jr.; Eaton, H. L.; Gemmecker, G.; Olejniczak, E. T.; Neri, P.; Holzman, T. F.; Egan, D. A.; Edalji, R.; Simmer, R.; Helfrich, R.; Hochlowski, J.; Jackson, M. *Biochemistry* **1991**, *30*, 6574–6583.

(23) (a) Karuso, P.; Kessler, H.; Mierke, D. F. *J. Am. Chem. Soc.* **1990**, *112*, 9434–9436. (b) Mierke, D. F.; Schmieder, P.; Karuso, P.; Kessler, H. *Helv. Chim. Acta* **1991**, *74*, 1027–1047. (c) van Duyne, G. D.; Standaert, R. F.; Karplus, P. A.; Schreiber, S. L.; Clardy, J. *Science* **1991**, *252*, 839–842.

(24) Seebach, D.; Thaler, A.; Beck, A. K. *Helv. Chim. Acta* **1989**, *72*, 857–867.

(25) (a) Thaler, A.; Seebach, D.; Cardinaux, F. *Helv. Chim. Acta* **1991**, *74*, 617–627. (b) Thaler, A.; Seebach, D.; Cardinaux, F. *Helv. Chim. Acta* **1991**, *74*, 628–643.

(26) (a) Pfeiffer, P.; von Modelski, J. *Hoppe-Seyler's Z. Physiol. Chem.* **1912**, *81*, 329–354. (b) Pfeiffer, P.; von Modelski, J. *Hoppe-Seyler's Z. Physiol. Chem.* **1913**, *85*, 1–34. (c) Pfeiffer, P. *Hoppe-Seyler's Z. Physiol. Chem.* **1924**, *133*, 22–61.

(27) (a) DeClercq, J. P.; Meulemans, R.; Piret, P.; van Meerssche, M. *Acta Crystallogr.* **1971**, *B27*, 539–544. (b) Meulemans, R.; Piret, P.; van Meerssche, M. *Acta Crystallogr.* **1971**, *B27*, 1187–1190. (c) Meulemans, R.; Piret, P.; van Meerssche, M. *Bull. Soc. Chim. Belg.* **1971**, *80*, 73–81. (d) Karle, I. L. *J. Am. Chem. Soc.* **1974**, *96*, 4000–4006. (e) Takahashi, N.; Tanaka, I.; Yamane, T.; Ashida, T.; Sugihara, T.; Imanishi, Y.; Higashimura, T. *Acta Crystallogr.* **1977**, *B33*, 2132–2136.

(28) Kessler, H.; Hehlein, W.; Schuck, R. *J. Am. Chem. Soc.* **1982**, *104*, 4534–4540. See also, gas-phase study of complexes of peptides and alkali metal ions: Teesch, L. M.; Orlando, R. C.; Adams, J. *J. Am. Chem. Soc.* **1991**, *113*, 3668–3675.

(29) Seebach, D. *Angew. Chem., Int. Ed. Engl.* **1988**, *27*, 1624–1654.

(30) (a) Gründler, H. Dissertation No. 9171, ETH Zürich, 1990. (b) Seebach, D.; Bossler, H.; Gründler, H.; Shoda, S.; Wenger, R. *Helv. Chim. Acta* **1991**, *74*, 197–224.

(31) Gerber, C.; Seebach, D. *Helv. Chim. Acta* **1991**, *74*, 1373–1385.

(32) Kofron, J. L.; Kuzmič, P.; Kishore, V.; Colón-Bonilla, E.; Rich, D. *Biochemistry* **1991**, *30*, 6172–6134.

(33) Kofron, J. L.; Kuzmič, P.; Kishore, V.; Gemmecker, G.; Fesik, S. W.; Rich, D. *J. Am. Chem. Soc.*, preceding paper in this issue.

(34) Köck, M.; Kessler, H. Complexation effects on the conformation of Cyclosporin A; the complex with lithium. Poster presentation in the 4th Chianti Workshop on Magnetic Resonance, June 2–8, 1991, San Miniato (Pisa), Italy.

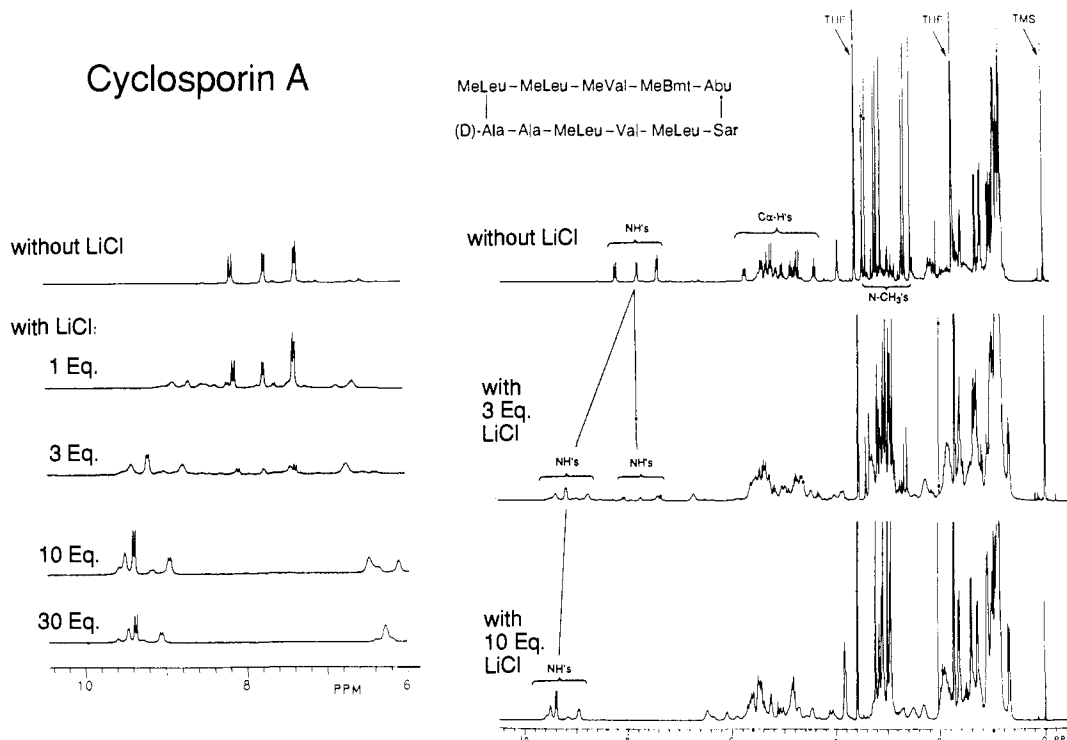(35) Köck, M. Diploma Thesis, Frankfurt/Main, 1989.

## Cyclosporin A

MeLeu – MeLeu – MeVal – MeBmt – Abu

(D)-Ala – Ala – MeLeu – Val – MeLeu – Sar



**Figure 2.** ^{1}H NMR spectrum of CsA in THF-$d_8$ upon addition of up to 30 equiv of LiCl. One conformation predominates without and with large amounts of LiCl. At intermediate concentrations, several conformers are present which equilibrate with each other slowly on the NMR time scale.

the signals to the chemical constitution of CsA in THF-$d_8$ with and without addition of LiCl. The 1D proton spectra of CsA in CDCl$_3$ and free and complexed in THF-$d_8$ are shown in Figure 3. While the first two are similar, the Li·CsA spectrum shows many distinct differences. A second conformation with a population of ~5% is visible in the 1D ^{1}H spectrum of the lithium-complexed CsA. The minor isomer was not studied further. The assignment procedure of the protons was carried out by standard procedures[20] via DQF-COSY[37] and TOCSY[38] spectra. A dramatic change in the proton chemical shifts of MeLeu[9] and Me-Leu[10] was observed (see Table I). The methyl groups of all MeLeu residues are separated in the uncomplexed CsA, whereas in the complex the chemical shifts of the methyl groups of MeLeu[6] and MeLeu[9] are degenerated. The problem in assigning the resonances of MeBmt[1] for CsA in THF-$d_8$ was the degeneracy of the C$_\beta$H and O$H$. The proof of the identical resonance frequency was carried out by variation of the temperature, using the larger temperature dependence of the chemical shift of the hydroxyl proton. In the case of Li·CsA, another problem occurs in assigning the resonances of the MeBmt[1] residue. The signals at 5.50 and 6.09 ppm show only one correlation: both are correlated to the C$_\beta$H proton and are assigned as the C$_\alpha$H and O$H$ protons. It was possible to distinguish them by a ROESY[39] spectrum: only the O$H$ signal shows an exchange peak to the water signal. After the assignment of all proton resonances, the sequential assignment was carried out with heteronuclear long-range couplings via HMBC[40] and verified by a NOESY[41] spectrum. The assignments
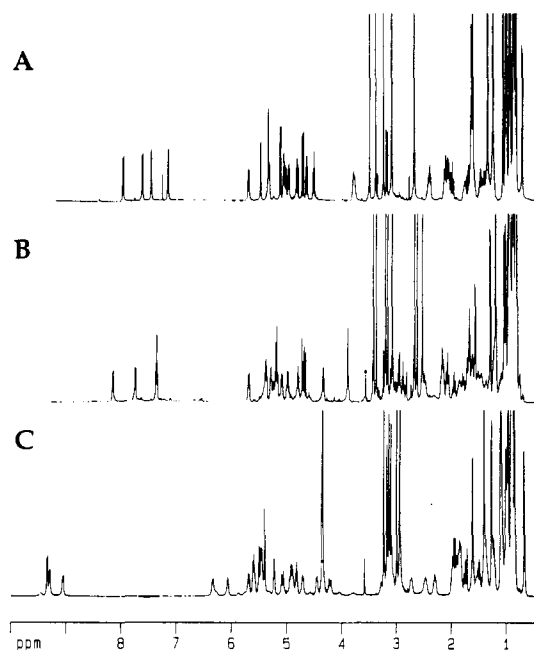


**Figure 3.** The 500-MHz ^{1}H NMR spectra of CsA in CDCl$_3$ (A), THF-$d_8$ (B), and THF-$d_8$ with addition of 30.9 equiv of LiCl (C).

of all proton resonances of the uncomplexed and complexed CsA in THF-$d_8$ are given in Table I.

For the assignment of the proton-bearing carbon atoms in the lithium complex, a HMQC[42] and a DEPT-HMQC[43] with TOCSY

(36) (a) Ernst, R. R.; Bodenhausen, G.; Wokaun, A. *Principles of Nuclear Magnetic Resonance in One and Two Dimensions*; Claredon Press: Oxford, UK, 1987. (b) Kessler, H.; Gehrke, M.; Griesinger, C. *Angew. Chem., Int. Ed. Engl.* **1988**, *27*, 490–536.

(37) Piantini, U.; Sørensen, O. W.; Ernst, R. R. *J. Am. Chem. Soc.* **1982**, *104*, 6800–6801.

(38) (a) Braunschweiler, L.; Ernst, R. R. *J. Magn. Reson.* **1983**, *53*, 521–528. (b) Bax, A.; Davis, D. G. *J. Magn. Reson.* **1985**, *65*, 355–360.

(39) (a) Bothner-By, A. A.; Stephens, R. L.; Lee, J.; Warren, C. D.; Jeanloz, R. W. *J. Am. Chem. Soc.* **1984**, *106*, 811–813. (b) Bax, A.; Davis, D. G. *J. Magn. Reson.* **1985**, *63*, 207–213. (c) Kessler, H.; Griesinger, C.; Kerssebaum, R.; Wagner, K.; Ernst, R. R. *J. Am. Chem. Soc.* **1987**, *109*, 607–609.

(40) (a) Bax, A.; Summers, M. F. *J. Am. Chem. Soc.* **1986**, *108*, 2093–2094. (b) Bax, A.; Marion, D. *J. Magn. Reson.* **1988**, *78*, 186–191.

(41) Jeener, J.; Meier, B. H.; Bachmann, P.; Ernst, R. R. *J. Chem. Phys.* **1979**, *71*, 4546–4553.

(42) (a) Müller, L. *J. Am. Chem. Soc.* **1979**, *101*, 4481–4484. (b) Bendall, M. R.; Pegg, D. T.; Doddrell, D. M. *J. Magn. Reson.* **1983**, *52*, 81–117. (c) Bax, A.; Griffey, R. H.; Hawkins, B. L. *J. Am. Chem. Soc.* **1983**, *105*, 7188–7190. (d) Bax, A.; Griffey, R. H.; Hawkins, B. L. *J. Magn. Reson.* **1983**, *55*, 301–315.

(43) Kessler, H.; Schmieder, P.; Kurz, M. *J. Magn. Reson.* **1989**, *85*, 400–405.

**Table I.** ^{1}H NMR Chemical Shifts of the Lithium-Complexed CsA Compared to CsA in THF-$d_8$, in CDCl$_3$, and Bound to Cyclophilin (CsA·CyP)[a]

| residue no. | amino acid | signal | Li-CsA[b] 300 K | CsA[b] (THF-$d_8$) 300 K | CsA[b] (THF-$d_8$) 250 K | CsA[b] (CDCl$_3$) 300 K | CsA·CyP[b] 293 K |
|---|---|---|---|---|---|---|---|
| 1 | MeBmt | NMe | 3.10 | 3.43 | 3.41 | 3.52 | 3.28 |
| | | C$_\alpha$H | 5.50 | 5.30 | 5.19 | 5.45 | 6.82 |
| | | C$_\beta$H | 4.71 | 3.89 | 3.89 | 3.82 | 4.04 |
| | | OH | 6.09 | 3.89 | 4.38 | 3.87 | |
| | | C$_\gamma$H | 1.55 | 1.69 | 1.72 | 1.63 | 1.50 |
| | | C$_\gamma$Me | 2.73 | 2.16 | 2.05 | 0.72 | 1.14 |
| | | C$_\delta$H | 1.83 | 1.79 | 1.75 | 2.41 | 2.60 |
| | | C$_\delta$H' | 0.83 | 0.83 | 0.85 | 1.73 | 2.25 |
| | | C$_\epsilon$H | 5.60 | 5.40 | 5.39 | 5.36 | 5.46 |
| | | C$_\zeta$H | 5.40 | 5.24 | 5.20 | 5.35 | 6.15 |
| | | C$_\eta$H | 1.60 | 1.57 | 1.57 | 1.62 | 1.61 |
| 2 | Abu | NH | 9.30 | 8.15 | 8.52 | 7.93 | 6.42[d] |
| | | C$_\alpha$H | 4.44 | 4.99 | 4.94 | 5.03 | 5.02 |
| | | C$_\beta$H | 2.48 | 1.68 | 1.80 | 1.75 | 1.65 |
| | | C$_\beta$H' | 1.83 | 1.68 | 1.61 | 1.64 | 1.45 |
| | | C$_\gamma$H | 1.08 | 0.83 | 0.84 | 0.87 | 0.67 |
| 3 | Sar | NMe | 3.17 | 3.38 | 3.39 | 3.40 | 2.93 |
| | | C$_\alpha$H | 5.05 | 4.67 | 4.65 | 4.76 | 5.31 |
| | | C$_\alpha$H' | 4.23 | 3.24 | 3.27 | 3.23 | 3.04 |
| 4 | MeLeu | NMe | 3.14 | 3.09 | 3.12 | 3.11 | 2.84 |
| | | C$_\alpha$H | 5.46 | 5.37 | 5.43 | 5.34 | 5.15 |
| | | C$_\beta$H | 1.89 | 1.95 | 1.91 | 2.00 | 1.68 |
| | | C$_\beta$H' | 1.35 | 1.62 | 1.70 | 1.64 | 1.57 |
| | | C$_\gamma$H | 1.39 | 1.46 | 1.43 | 1.44 | 1.38 |
| | | C$_\delta$H | 0.97 | 0.93 | 0.94 | 0.95 | 0.93 |
| | | C$_\delta$H' | 0.90 | 0.87 | 0.86 | 0.88 | 0.88 |
| 5 | Val | NH | 9.06 | 7.37 | 7.45 | 7.47 | 8.53 |
| | | C$_\alpha$H | 4.93 | 4.71 | 4.72 | 4.67 | 4.30 |
| | | C$_\beta$H | 1.84 | 2.48 | 2.50 | 2.41 | 2.02 |
| | | C$_\gamma$H | 1.09 | 1.02 | 1.00 | 1.06 | 0.94 |
| | | C$_\gamma$H' | 0.89 | 0.83 | 0.79 | 0.90 | 0.93 |

| residue no. | amino acid | signal | Li-CsA[b] 300 K | CsA[b] (THF-$d_8$) 300 K | CsA[b] (THF-$d_8$) 250 K | CsA[b] (CDCl$_3$) 300 K | CsA·CyP[b] 293 K |
|---|---|---|---|---|---|---|---|
| 6 | MeLeu | NMe | 3.23 | 3.21 | 3.22 | 3.25 | 3.09 |
| | | C$_\alpha$H | 5.45 | 5.18 | 5.22 | 5.02 | 5.42 |
| | | C$_\beta$H | 1.95 | 2.07 | 2.14 | 2.06 | 1.82 |
| | | C$_\beta$H' | 1.73 | 1.22 | 1.08 | 1.41 | 1.73 |
| | | C$_\gamma$H | 1.22 | 1.86 | 1.96 | 1.76 | 1.60 |
| | | C$_\delta$H | 0.87 | 0.93 | 0.94 | 0.94 | 0.89 |
| | | C$_\delta$H' | 0.87 | 0.81 | 0.74 | 0.85 | 0.78 |
| 7 | Ala | NH | 6.32 | 7.74 | 8.09 | 7.75 | 7.56 |
| | | C$_\alpha$H | 4.89 | 4.34 | 4.33 | 4.52 | 4.20 |
| | | C$_\beta$H | 1.26 | 1.30 | 1.28 | 1.36 | 1.39 |
| 8 | D-Ala | NH | 9.33 | 7.35 | 7.60 | 7.18 | 8.33 |
| | | C$_\alpha$H | 4.81 | 4.80 | 4.76 | 4.84 | 4.68 |
| | | C$_\beta$H | 1.39 | 1.20 | 1.21 | 1.26 | 1.16 |
| 9 | MeLeu | NMe | 2.93 | 3.17 | 3.04 | 3.12 | 2.61 |
| | | C$_\alpha$H | 5.22 | 5.69 | 5.65 | 5.70 | 5.19 |
| | | C$_\beta$H | 1.98 | 2.07 | 2.18 | 2.13 | 1.13 |
| | | C$_\beta$H' | 1.22 | 1.20 | 1.09 | 1.25 | -0.15 |
| | | C$_\gamma$H | 1.49 | 1.37 | 1.38 | 1.32 | 0.77 |
| | | C$_\delta$H | 0.86 | 0.94 | 0.94 | 0.97 | 0.54 |
| | | C$_\delta$H' | 0.86 | 0.88 | 0.85 | 0.89 | 0.32 |
| 10 | MeLeu | NMe | 2.93 | 2.64 | 2.61 | 2.70 | 2.83 |
| | | C$_\alpha$H | 5.68 | 5.09 | 5.15 | 5.10 | 5.98 |
| | | C$_\beta$H | 1.92 | 2.18 | 2.17 | 2.13 | 1.55 |
| | | C$_\beta$H' | 1.42 | 1.11 | 1.07 | 1.24 | 1.47 |
| | | C$_\gamma$H | 1.61 | 1.53 | 1.48 | 1.49 | 1.45 |
| | | C$_\delta$H | 1.07 | 1.05 | 1.09 | 0.98 | 1.10 |
| | | C$_\delta$H' | 0.95 | 0.97 | 0.99 | 0.98 | 1.10 |
| 11 | MeVal | NMe | 2.99 | 2.68 | 2.64 | 2.71 | 2.73 |
| | | C$_\alpha$H | 5.59 | 5.20 | 5.19 | 5.15 | 4.55 |
| | | C$_\beta$H | 2.29 | 2.18 | 2.18 | 2.17 | 1.47 |
| | | C$_\gamma$H | 0.99 | 0.93 | 0.91 | 1.01 | 0.47 |
| | | C$_\gamma$H' | 0.66 | 0.83 | 0.83 | 0.87 | -0.69 |

[a] All data are given in ppm. The prime (*H'*) indicates the high-field proton. [b] The chemical shifts values are obtained from spectra with 2048 data points. [c] Data taken from ref 19c. [d] Data taken from ref 19b.

2680  *J. Am. Chem. Soc., Vol. 114, No. 7, 1992*

*Köck et al.*

**Table II.** $^{13}$C NMR Chemical Shifts of the Lithium-Complexed CsA Compared to CsA in THF-$d_8$, in CDCl$_3$, and Bound to Cyclophilin (CsA·CyP)$^a$

| residue no. | amino acid | group | Li·CsA | CsA (THF-$d_8$) | CsA (CDCl$_3$) | CsA·CyP$^b$ | residue no. | amino acid | group | Li·CsA | CsA (THF-$d_8$) | CsA (CDCl$_3$) | CsA·CyP$^b$ |
|---|---|---|---|---|---|---|---|---|---|---|---|---|---|
| 1 | MeBmt | CO | 173.87 | 170.28 | 169.65 | 172.4 | 6 | MeLeu | CO | 172.84 | 172.07 | 170.87 | 171.9 |
| | | NMe | 36.47 | 33.26 | 33.97 | 34.4 | | | NMe | 33.35 | 31.64 | 31.53 | 31.8 |
| | | C$_a$ | 60.66 | 59.55 | 58.75 | 58.1 | | | C$_\alpha$ | 57.46 | 55.63 | 55.31 | 54.8 |
| | | C$_\beta$ | 74.95 | 73.76 | 74.74 | 75.7 | | | C$_\beta$ | 40.41 | 38.14 | 37.41 | 37.0 |
| | | C$_\gamma$ | 38.02 | 35.25 | 35.99 | 25.0 | | | C$_\gamma$ | 25.23 | 25.83 | 25.40 | 24.0 |
| | | C$_\gamma$Me | 15.79 | 18.06 | 16.76 | 15.1 | | | C$_\delta$ | 23.57 | 24.67 | 23.87 | 22.4 |
| | | C$_\delta$ | 37.20 | 34.93 | 35.63 | 34.0 | | | C$_\delta'$ | 21.72 | 22.24 | 21.93 | 19.8 |
| | | C$_\epsilon$ | 132.39 | 131.98 | 129.68 | 124.3 | 7 | Ala | CO | 172.69 | 171.60 | 170.44 | 173.2 |
| | | C$_\zeta$ | 125.83 | 125.62 | 126.32 | 130.1 | | | C$_\alpha$ | 49.54 | 49.12 | 48.69 | 49.3 |
| | | C$_\eta$ | 18.28 | 18.06 | 17.96 | 17.2 | | | C$_\beta$ | 18.03 | 15.87 | 16.07 | 17.0 |
| 2 | Abu | CO | 175.43 | 174.15 | 173.04 | 172.0 | 8 | D-Ala | CO | 175.51 | 174.79 | 172.87 | 175.1 |
| | | C$_\alpha$ | 55.73 | 49.50 | 48.86 | 50.7 | | | C$_\alpha$ | 46.19 | 45.64 | 45.20 | 45.3 |
| | | C$_\beta$ | 23.07 | 25.97 | 25.06 | 24.4 | | | C$_\beta$ | 15.96 | 18.06 | 18.19 | 15.5 |
| | | C$_\gamma$ | 11.96 | 10.39 | 9.93 | 9.8 | 9 | MeLeu | CO | 170.84 | 170.84 | 169.75 | 171.2 |
| 3 | Sar | CO | 170.03 | 172.17 | 170.50 | 170.6 | | | NMe | 30.71 | 29.73 | 29.65 | 29.2 |
| | | NMe | 36.69 | 39.25 | 39.40 | 33.7 | | | C$_\alpha$ | 54.56 | 48.84 | 48.30 | 52.1 |
| | | C$_\alpha$ | 51.34 | 50.38 | 50.37 | 50.9 | | | C$_\beta$ | 39.02 | 40.19 | 39.04 | 36.4 |
| 4 | MeLeu | CO | 170.03 | 170.09 | 169.35 | 171.1 | | | C$_\gamma$ | 25.86 | 25.56 | 24.70 | 22.6 |
| | | NMe | 30.71 | 31.38 | 31.32 | 29.3 | | | C$_\delta$ | 22.93 | 23.74 | 23.74 | 23.2 |
| | | C$_\alpha$ | 54.84 | 55.99 | 55.51 | 53.8 | | | C$_\delta'$ | 21.38 | 22.42 | 21.86 | 20.2 |
| | | C$_\beta$ | 39.28 | 36.80 | 35.99 | 36.0 | 10 | MeLeu | CO | 174.45 | 170.43 | 169.41 | 173.1 |
| | | C$_\gamma$ | 25.72 | 25.65 | 24.90 | 23.8 | | | NMe | 31.68 | 29.84 | 29.83 | 32.2 |
| | | C$_\delta$ | 22.68 | 24.08 | 23.49 | 21.5 | | | C$_\alpha$ | 50.80 | 57.94 | 57.54 | 52.9 |
| | | C$_\delta'$ | 23.78 | 21.65 | 21.18 | 21.8 | | | C$_\beta$ | 38.75 | 41.95 | 40.73 | 36.9 |
| 5 | Val | CO | 177.02 | 174.52 | 173.07 | 174.9 | | | C$_\gamma$ | 26.27 | 25.56 | 24.55 | 25.0 |
| | | C$_\alpha$ | 55.57 | 55.77 | 55.39 | 56.4 | | | C$_\delta$ | 23.78 | 23.95 | 23.85 | 23.5 |
| | | C$_\beta$ | 31.68 | 32.23 | 31.17 | 29.4 | | | C$_\delta'$ | 21.61 | 24.48 | 23.38 | 19.1 |
| | | C$_\gamma$ | 20.50 | 20.07 | 19.81 | 18.2 | 11 | MeVal | CO | 170.84 | 173.81 | 172.85 | 170.5 |
| | | C$_\gamma'$ | 18.69 | 18.74 | 18.48 | 19.4 | | | NMe | 31.18 | 30.81 | 29.81 | 33.2 |
| | | | | | | | | | C$_\alpha$ | 60.54 | 58.49 | 57.93 | 59.3 |
| | | | | | | | | | C$_\beta$ | 27.81 | 30.12 | 29.05 | 24.7 |
| | | | | | | | | | C$_\gamma$ | 21.01 | 19.18 | 18.75 | 18.8 |
| | | | | | | | | | C$_\gamma'$ | 17.97 | 20.37 | 20.26 | 16.3 |

$^a$All data are given in ppm. The prime ($C'$) indicates the carbon of the high-field proton. If the proton chemical shifts are degenerated the low-field carbon is mentioned first (without prime). $^b$The assignments are from different inverse correlation heteronuclear experiments, but the chemical shifts reported are from the one-dimensional $^{13}$C spectrum. $^c$Data taken from ref 19b.

transfer[44] were used. With the aid of DEPT[45] editing techniques (using the multiquantum coherence terms[46]), it is possible to select certain multiplicities (CH, CH$_2$, and CH$_3$) using different editing pulse lengths. Starting with a chemical shift of a previously assigned proton, usually the whole $^{13}$C spin system of the amino acid is depicted on a line parallel to the $F_1$ axis in the spectrum with TOCSY transfer. For the unambiguous assignment of the methyl groups, a HQQC[47] experiment was used. The carbonyl and N-methyl carbons were assigned by the HMBC spectrum. All carbon chemical shifts of the uncomplexed and complexed CsA in THF-$d_8$ are given in Table II.

To determine high-quality conformations it is desirable to assign the geminal protons and the geminal methyl groups of MeLeu and (Me)Val diastereotopically. For the geminal $\beta$-protons this was achieved with homonuclear coupling constants from an E. COSY[48] spectrum and qualitative evaluation of the C$_\beta$H–C′ cross peaks from the HMBC following a procedure described in the literature.[49] These assignments were checked by NOE effects,[50] and no ambiguities were found. The diastereotopic assignment of the Sar$^3$C$_\alpha$H protons was carried out with interproton distances derived from the NOESY spectra and a structure obtained from

**Table III.** Diastereotopically Assigned Protons and Methyl Groups of Li·CsA in Comparison to CsA in CDCl$_3$$^a$

| | Li·CsA | | CsA | |
|---|---|---|---|---|
| residue | $H(Me)$ | $H'(Me')$ | $H(Me)$ | $H'(Me')$ |
| MeBmt$^1$($\delta$) | $H^{Re}$ | $H^{Si}$ | $H^{Re}$ | $H^{Si}$ |
| Abu$^2$($\beta$) | $H^{Re}$ | $H^{Si}$ | $H^{Si}$ | $H^{Re}$ |
| Sar$^3$($\alpha$) | $H^{Si}$ | $H^{Re}$ | $H^{Si}$ | $H^{Re}$ |
| MeLeu$^4$($\beta$) | $H^{Re}$ | $H^{Si}$ | $H^{Si}$ | $H^{Re}$ |
| MeLeu$^4$($\delta$) | $Me^{Re}$ | $Me^{Si}$ | $Me^{Re}$ | $Me^{Si}$ |
| Val$^5$($\gamma$) | $Me^{Re}$ | $Me^{Si}$ | $Me^{Si}$ | $Me^{Si}$ |
| MeLeu$^6$($\beta$) | $H^{Si}$ | $H^{Re}$ | $H^{Si}$ | $H^{Re}$ |
| MeLeu$^6$($\delta$) | | | $Me^{Si}$ | $Me^{Re}$ |
| MeLeu$^9$($\beta$) | $H^{Si}$ | $H^{Re}$ | $H^{Re}$ | $H^{Si}$ |
| MeLeu$^9$($\delta$) | | | $Me^{Re}$ | $Me^{Si}$ |
| MeLeu$^{10}$($\beta$) | $H^{Re}$ | $H^{Si}$ | $H^{Re}$ | $H^{Si}$ |
| MeLeu$^{10}$($\delta$) | $Me^{Re}$ | $Me^{Si}$ | | |
| MeVal$^{11}$($\gamma$) | $Me^{Re}$ | $Me^{Si}$ | $Me^{Re}$ | $Me^{Si}$ |

$^a$$H$ or $Me$ signed by primes indicate the high-field proton or methyl group.

a MD simulation carried out without diastereotopic assignments. In this crude model, the assignment was based on chemical shift arguments and distances: the chemical shift of the C$_\alpha$H proton in the plane of the carbonyl carbon is shifted downfield compared to the other proton. This is confirmed by the results from interproton distances. The assignment of the diastereotopic methyl groups of Val$^5$ and MeVal$^{11}$ was easily obtained, because the $^3J_{C_\alpha H, C_\beta H}$ couplings were larger than 10 Hz, only consistent with $\chi_1 = -60°$ rotamer. Assuming this side-chain conformation, the NOE effect to the neighboring N-methyl groups led to the assignment of the methyl groups. The C$_\delta$H of MeBmt$^1$ and C$_\delta$Me of MeLeu$^4$ and MeLeu$^{10}$ were diastereotopically assigned via NOE effects. For the degenerated MeLeu$^6$C$_\delta$Me and MeLeu$^9$C$_\delta$Me signals, no diastereotopic assignment was possible. The diaste-

(44) Lerner, A.; Bax, A. *J. Magn. Reson.* **1986**, *69*, 375–380.

(45) Doddrell, D. M.; Pegg, D. T.; Bendall, M. R. *J. Magn. Reson.* **1982**, *48*, 323–327.

(46) Kessler, H.; Schmieder, P. *Biopolymers* **1991**, *31*, 621–629.

(47) Kessler, H.; Schmieder, P.; Köck, M.; Reggelin, M. *J. Magn. Reson.* **1991**, *91*, 375–379.

(48) (a) Griesinger, C.; Sørensen, O. W.; Ernst, R. R. *J. Am. Chem. Soc.* **1985**, *107*, 6394–6396. (b) Griesinger, C.; Sørensen, O. W.; Ernst, R. R. *J. Magn. Reson.* **1987**, *75*, 474–492.

(49) (a) Hofmann, M.; Bermel, W.; Gehrke, M.; Kessler, H. *Magn. Reson. Chem.* **1989**, *27*, 877–886. (b) Bermel, W.; Wagner, K.; Griesinger, C. *J. Magn. Reson.* **1989**, *83*, 223–232.

(50) Wagner, G.; Braun, W.; Havel, T. F.; Schaumann, T.; Go, N.; Wüthrich, K. *J. Mol. Biol.* **1987**, *196*, 611–639.

**Table IV.** $^3J(NH,C_\alpha H)$ Coupling Constants and Temperature Gradients of the Amide Protons of CsA in THF-$d_8$ with and without LiCl in Comparison to CsA in CDCl$_3$

| | coupling constants[a] | | | | temperature gradients[b] | | |
| --- | --- | --- | --- | --- | --- | --- | --- |
| | Li·CsA | CsA THF-$d_8$ | CsA (250 K) THF-$d_8$ | CsA[c] CDCl$_3$ | Li·CsA[d] | CsA[d] THF-$d_8$ | CsA[e] CDCl$_3$ |
| Abu[2] | 6.2[f] | 9.8 | 9.3 | 9.4 | 6.0 | 5.6 | 3.6 |
| Val[5] | 9.9 | 9.2 | 9.3 | 8.0 | 2.6 | 1.4 | 1.8 |
| Ala[7] | 8.0 | 7.0 | 6.2 | 8.0 | 1.0 | 5.0 | 3.6 |
| D-Ala[8] | 8.7 | 7.6 | 6.9 | 8.0 | 3.5 | 3.3 | 1.1 |

[a] Coupling constants in hertz are from one-dimensional proton spectra with a size of 16 384 data points given. [b] The temperature gradients are given in $-\Delta\delta/\Delta T$ (ppb·K$^{-1}$). [c] Data taken from ref 9b. [d] The temperature gradients have been measured between 300 and 330 K (in steps of 10 K). [e] The temperature gradients have been measured between 300 and 325 K (in steps of 5 K). [f] This coupling constant is obtained from a procedure described in ref 53.

**Table V.** $^3J(C_\alpha H,C_\beta H)$ Side-Chain Coupling Constants and Populations for the Side Chains[a]

| | Li·CsA | | | | | CsA in CDCl$_3$ | | | | |
| --- | --- | --- | --- | --- | --- | --- | --- | --- | --- | --- |
| | coupling constants | | populations | | | coupling constants | | populations | | |
| residue | $^3J_{C_\alpha H,C_\beta H}$ | $^3J_{C_\alpha H,C_\beta H'}$ | P$_I$ | P$_{II}$ | P$_{III}$ | $^3J_{C_\alpha H,C_\beta H}$ | $^3J_{C_\alpha H,C_\beta H'}$ | P$_I$ | P$_{II}$ | P$_{III}$ |
| MeBmt[1] | 4.4[b] | | | | | 6.3 | | | | |
| Abu[2] | 6.0 | 7.0 | 40 | 31 | 29 | 7.1 | 8.0 | 49 | 41 | 10 |
| MeLeu[4] | 6.5 | 5.4 | 25 | 36 | 39 | 4.2 | 11.8 | 84 | 14 | 2 |
| Val[5] | 10.2[c] | | ~100 | | | 10.2 | | ~100 | | |
| MeLeu[6] | 4.1 | 12.1 | 86 | 14 | 0 | 10.3 | 6.0 | 30 | 70 | 0 |
| MeLeu[9] | 8.0 | 6.5 | 36 | 49 | 15 | 11.2 | 4.6 | 78 | 18 | 4 |
| MeLeu[10] | 12.5 | 3.2 | 90 | 5 | 5 | 8.2 | 6.5 | 51 | 35 | 14 |
| MeVal[11] | 10.2[b] | | ~100 | | | 11.0 | | ~100 | | |

[a] The coupling constants (Hz) are obtained from the E. COSY spectrum. P$_I$, P$_{II}$, and P$_{III}$ represent $\chi_1$ values of $-60°$, $180°$, and $60°$, respectively. [b] Coupling constants are obtained from rows of the DQF-COSY (32 768 data points) with a method described in ref 53. [c] Similar to (b), but with modifications, because of the passive coupling involved in this cross peak in $F_2$.

reotopic assignments of the complex in comparison to those found for CsA in CDCl$_3$ are given in Table III.

**Extraction of Conformationally Relevant NMR Parameters.** The N$H$–C$_\alpha H$ coupling constants were extracted from a 1D spectrum after resolution enhancement (see Table IV). The C$_\alpha H$–C$_\beta H$ coupling constants, obtained from an E. COSY spectrum, are important to identify preferred orientation of the $\chi_1$ rotamers. The populations of different side-chain rotamers were determined via standard procedures,[51] under the assumption that only the three staggered rotamers around the C$_\alpha$–C$_\beta$ bond are populated.[52] Antiphase couplings have been determined using a procedure described in the literature.[53] The coupling constants and the side-chain rotamer populations of Li·CsA in comparison to CsA in CDCl$_3$ are given in Table V.

Temperature gradients were obtained from 1D spectra measured between 300 and 330 K (see Table IV). In contrast to the solvents DMSO[54] and CDCl$_3$,[55] not enough empirical data exist for a reliable discussion of the temperature dependence of amide proton chemical shifts in THF-$d_8$. Thus, no conclusion about external or internal orientation of amide protons can be made.

The NOESY spectrum of uncomplexed CsA in THF-$d_8$ at 500 MHz and 300 K showed only a few, very weak positive NOE effects and some antiphase signals (no zero-quantum suppression was used). This is to be expected since similar observations were made for CsA in CDCl$_3$ and the solvents have similar viscosities. Therefore, the NOESY spectrum was measured at a temperature of 250 K. This, of course, requires the assignment of the proton resonances at this temperature (see Table I). A detailed conformational analysis of CsA in THF-$d_8$ was not carried out because a comparison of $^{13}$C chemical shift values, as well as the qualitative interpretation of the NOE effects and homonuclear coupling constants, indicates a backbone conformation very similar to that observed in CDCl$_3$.[18]
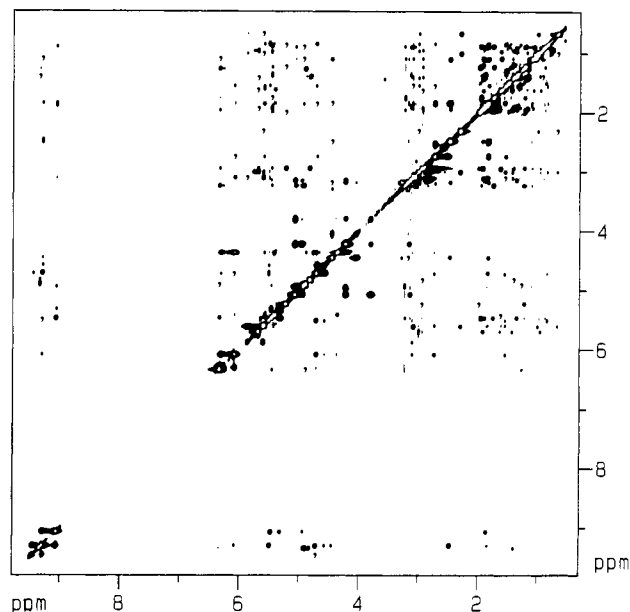
(51) Kessler, H.; Griesinger, C.; Wagner, K. *J. Am. Chem. Soc.* **1987**, *109*, 6927–6933.

(52) (a) Pachler, K. G. R. *Spectrochim. Acta* **1963**, *19*, 2085–2092. (b) Pachler, K. G. R. *Spectrochim. Acta* **1964**, *20*, 581–587.

(53) Kim, Y.; Prestegard, J. H. *J. Magn. Reson.* **1989**, *84*, 9–13.

(54) Kessler, H. *Angew. Chem., Int. Ed. Engl.* **1982**, *21*, 512–523.

(55) Stevens, E. S.; Sugawara, N.; Bonora, G. M.; Toniolo, C. *J. Am. Chem. Soc.* **1980**, *102*, 7048–7050.



**Figure 4.** The 600-MHz NOESY spectrum of lithium-complexed CsA in THF-$d_8$ at 300 K obtained with a mixing time of 200 ms.

For the quantitative analysis of the complex Li·CsA, NOESY buildup rates[56] were recorded at 300 K and 600 MHz with five different mixing times (40, 80, 120, 160, and 200 ms). The observation of NOEs indicates a considerably slower tumbling of the complex in comparison to the uncomplexed CsA, leading to strong NOE effects (see Figure 4). A ROESY spectrum was used to distinguish NOE and exchange peaks (different sign); therefore, the two sets of signals obtained in the 1D $^1$H spectrum were confirmed as conformers and not configurational isomers or a mixture of constitutional isomers. Some of these exchange peaks are very strong, indicating a fast exchange rate (see Figure

(56) (a) Kumar, A.; Wagner, G.; Ernst, R. R.; Wüthrich, K. *J. Am. Chem. Soc.* **1981**, *103*, 3654–3658. (b) Bodenhausen, G.; Ernst, R. R. *J. Am. Chem. Soc.* **1982**, *104*, 1304–1309.
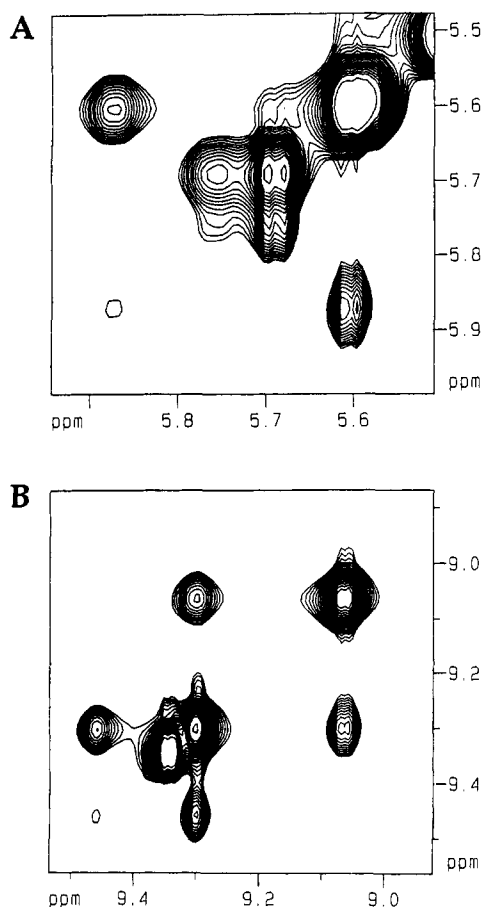
**Figure 5.** Exchange peaks in the (A) $C_\alpha H$ region and (B) amide region of the minor and major conformations of the lithium-complexed CsA, obtained from a 600-MHz NOESY spectrum at 300 K with a mixing time of 200 ms. Both parts of the spectrum were plotted with the same number of levels.

5). It is often observed that conformations with small populations are easily observed by strong exchange cross peaks. The exchange cross peak of the minor (9.45 ppm) and the major isomers (9.30 ppm) of Abu²NH indicates that the second conformation is also different from the normal CsA structure, because of its lowfield shift (see Figure 5). Assignment of some of the NOE cross peaks was difficult, because of degeneracy, or partial degeneracy, of some of the chemical shifts, for example, MeLeu⁴$C_\alpha H$/MeLeu⁶$C_\alpha H$ and especially for MeBmt¹$C_\xi H$/MeVal¹¹$C_\alpha H$ and MeLeu⁹N*Me*/MeLeu¹⁰N*Me*. The latter two provided special problems because of the proximity of these protons in the molecule. The integral intensities of the cross peaks were measured by the integration routine within the UXNMR program, after a third-order base-plane correction. In total, 130 NOE cross peaks (8 scaling, 77 intraresidual, 38 interresidual, and 6 long-range peaks) were obtained. In comparison to CsA in CDCl₃ and THF-$d_8$, the lithium complex shows only a few long-range NOEs.[18] First the NOE data were transformed into distances under the approximation of a rigid molecule with isotropic molecular reorientation. The isolated two-spin approximation may result in significant systematic deviation from actual distances, especially for longer distances. These effects become more severe with increasing correlation times. One method to avoid the isolated two-spin approximation, is the full relaxation matrix method.[57] Therefore, the intensities of the NOESY spectra were used in an iterative relaxation matrix approach (IRMA).[58] For calibration of the NOESY integrals, the cross peak SarC$_\alpha H$/SarC$_\alpha H'$ was used. The intensity of this integral was scaled to 178 pm, leading to a

good agreement with other fixed distances, including other geminal protons and AlaC$_\alpha H$,C$_\beta H$ or (Me)ValC$_\beta H$,C$_\gamma H$ (240 pm).

The ¹³C $T_1$ relaxation times with 10 different delays (50, 100, 150, 200, 300, 400, 500, 750, 1000, and 1500 ms) were measured for the complex at 125.76 MHz. The 1D inversion–recovery method was used with a long relaxation delay (10 s) and proton decoupling during the whole sequence necessary for a quantitative interpretation of the relaxation times. The peaks were integrated and fitted with a three-parameter least-squares fit using software supplied by Bruker. The relaxation times of the C$_\alpha$ carbons were averaged (280 ms) and used for the determination of the correlation time,[59] following the formula

$$1/T_1 = \rho_s = nW_0 + 2W_1 + nW_2 =$$
$$C\{n[\tau_c/(1 + (\omega_1 - \omega_s)^2)\tau_c^2] + 3[\tau_c/(1 + (\omega_s)^2)\tau_c^2] +$$
$$6n[\tau_c/(1 + (\omega_1 + \omega_s)^2)\tau_c^2]\}$$

where $C$ is

$$C = h^2\gamma_1^2\gamma_s^2\mu_0^2/(10r^6(4\pi)) = 2.1324 \times 10^{-9}$$

$n$ is number of protons and other symbols have their standard meaning. When only one field strength is used, two solutions are obtained from this formula. Normally one value can be excluded by comparison with the signs of the cross peaks observed in the NOESY spectrum. The calculated values are 0.3 and 2.7 ns; the former can be discarded because of the negative NOE effects.

**Conformational Analysis.** The NOESY spectrum of the uncomplexed CsA in pure THF-$d_8$ shows the same characteristic cross-peak pattern as found for CsA in CDCl₃, for example, the important cross peaks MeLeu⁹$C_\alpha H$–MeLeu¹⁰$C_\alpha H$ and MeBmt¹$C_\alpha H$–MeLeu⁶$C_\alpha H$. Again in contrast, the NOESY of the lithium-complexed CsA exhibits no C$_\alpha$H–C$_\alpha$H cross peak between neighboring amino acids, but all N$H$–C$_\alpha H$ or N*Me*–C$_\alpha H$ were recognized, leading to the conclusion that no cis peptide bond is present in the complex. In addition, the MeBmt¹$C_\alpha H$–MeLeu⁶$C_\alpha H$ cross peak typical for the $\beta$ sheet is missing. All N$H$–N$H$ cross peaks are exchange peaks and therefore none of the amide protons are involved in hydrogen bonds, whereas in CDCl₃ all amide protons are involved in internal hydrogen bonds. No exchange cross peak is found for the correlation between MeBmt¹OH and Abu²NH.

Comparing the lithium complex with the uncomplexed CsA in CDCl₃, an evaluation of $^3J_{C_\alpha H, C_\beta H}$ coupling constants indicates that all populations of the MeLeu side chains have changed: e.g., the side chain of MeLeu¹⁰ in CDCl₃ populates more than one conformation, whereas in the Li complex, it adopts a clear preference (90%) for the P₁ ($X_1 = -60°$) rotamer. For MeLeu⁹ the opposite case was obtained: in CsA in CDCl₃ the P₁ rotamer dominates (78%), whereas for Li·CsA, a nearly identical population of P₁ and P₁₁ was obtained (see Table V).

**Structure Refinement by Molecular Dynamics (MD) Simulations**

To translate the interproton distances and additional experimental parameters into a three-dimensional molecular structure, restrained and unrestrained MD simulations[60] using the GROMOS[61] program were utilized. The generation of the starting structure and interactive modeling was carried out with the program INSIGHT (Biosym). All calculations were performed on Silicon Graphics 4D/25TG, 4D/70GTB, and 4D/240SX computers. No parameters for THF are available; therefore, all MD calculations were carried out in vacuo. The SHAKE[62] algorithm with a relative tolerance of $10^{-4}$ nm and a time step of 2 fs for the numerical integration of Newton's equation was used in the MD runs. A

(57) Keepers, J. W.; James, T. L. *J. Magn. Reson.* **1984**, *57*, 404–426.

(58) (a) Boelens, R.; Koning, T. M. G.; Kaptein, R. *J. Mol. Struct.* **1988**, *173*, 299–311. (b) Boelens, R.; Koning, T. M. G.; van der Marel, G. A.; van Boom, J. H.; Kaptein, R. *J. Magn. Reson.* **1989**, *82*, 290–308.

(59) Clore, G. M.; Driscoll, P. C.; Wingfield, P. T.; Gronenborn, A. M. *Biochemistry* **1990**, *29*, 7387–7401.

(60) van Gunsteren, W. F.; Berendsen, H. J. C. *Angew. Chem., Int. Ed. Engl.* **1990**, *29*, 992–1023.

(61) Biomos B. V.: Nijenborgh 16 NL 9747 AG Groningen, Groningen Molecular Simulation (GROMOS) Library Manual, van Gunsteren, W. F., Berendsen, H. J. C., Eds.; *GROMOS User Manual*, pp 1–229.

(62) (a) Ryckaert, J. P.; Cicotti, C.; Berendsen, H. J. C. *J. Comput. Phys.* **1977**, *23*, 327–343. (b) van Gunsteren, W. F.; Berendsen, H. J. C. *Mol. Phys.* **1977**, *34*, 1311–1327.
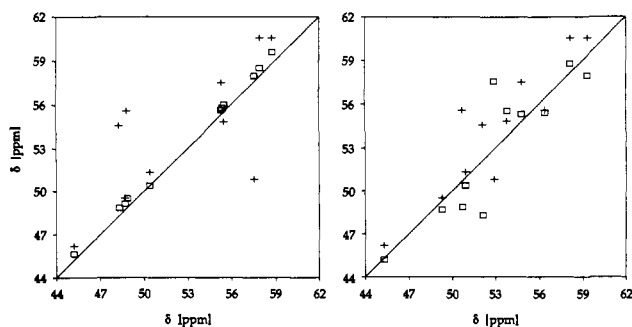
**Figure 6.** Comparison of the chemical shifts of the $C_\alpha$ carbons of CsA in $CDCl_3$ to CsA in THF-$d_8$ and the lithium complex (left): CsA in $CDCl_3$ to CsA in THF-$d_8$ (squares) and CsA in $CDCl_3$ to Li·CsA in THF-$d_8$ (crosses). The comparison of the $C_\alpha$ carbons of CyP·CsA to CsA in $CDCl_3$ and the lithium complex is shown on the right: CsA·CYP to CsA in $CDCl_3$ (squares) and CsA·CYP to Li·CsA in THF-$d_8$ (crosses).

dielectric permittivity of 1 was used for all calculations. The cutoff radius for the nonbonded interactions was set to 10 nm to include all atom–atom interactions. The velocities, given to the atoms initially, were taken from a Maxwellian distribution.

A starting structure was built interactively and energy minimized with the steepest descents algorithm,[63] to remove any strain caused by covalent distorsions. All peptide bonds were assumed to be trans. Because some of the dihedral angles of the peptide bonds were found to deviate considerably from 180°, 20 ps of MD at 1000 K with dihedral restraining of the peptide bonds was carried out. The resulting structure was energy minimized with conjugate gradients (see Figure 7a).[64]

The MD calculations were run in combination with the iterative relaxation matrix approach to take spin-diffusion (indirect magnetization transfer) into account. Since spin-diffusion has a greater effect on longer distances, the range (and the number) of the distance restraints can be extended with the use of IRMA. A pseudoatom correction of 30 pm[65] for the upper bond of methyl groups was used. The upper and lower distance bounds were set to plus and minus 10% of the calculated distances. This variation allows for some error in the measurement of the intensity of cross peaks and the conversion to distances. The calculations were started with 83 assigned intensities, including calibration peaks, from the NOESY spectra.

An example MD simulation after an IRMA cycle consisted of 20 ps at 1000 K with a force constant ($k_{dr}$) of 2000 kJ mol$^{-1}$ nm$^{-2}$ for the restraining potential of the NOE-derived distances. The temperature and $k_{dr}$ were then reduced to 300 K and 1000 kJ mol$^{-1}$ nm$^{-2}$, respectively, and the simulation continued for 100 ps. The high-temperature part was only carried out for the first IRMA cycle. Every picosecond 10 structures were stored in order to get a reasonable ensemble of conformations for averaging. The structure averaged over 60 ps, from 60 to 120 ps, was energy minimized using the conjugate gradients algorithm with a $k_{dr}$ of 1000 kJ mol$^{-1}$ nm$^{-2}$. The obtained structure was then used to start the next IRMA cycle.

## Results and Discussion

It is evident from Figure 6 (left) that the chemical shift values of all $\alpha$-carbons are very similar in $CDCl_3$ and THF-$d_8$ (indicated by squares in this figure). As carbon chemical shifts are strongly determined by the conformation,[66] it is obvious that no conformational change in the backbone was induced by changing the solvent from $CDCl_3$ to THF-$d_8$. If one compares the effect of the addition of lithium chloride in the same manner, a large

difference is evident (crosses), indicating a conformational change. In Figure 6 (right) the chemical shifts are compared with those of the complex with cyclophilin (CsA·CyP): it is evident that the lithium complex is conformationally different from bound CsA.

The $^{13}$C $T_1$ relaxation times of the carbonyl carbons give a rough indication of the position of the lithium ion; the carbonyls of Abu$^2$, Sar$^3$, MeLeu$^4$ (the latter two are degenerated), and MeLeu$^{10}$ have significant shorter relaxation times. This may be an effect of the interaction with the lithium ion or a restricted mobility due to complexation. From preliminary calculations *including the lithium ion*, it can be concluded that CsA is complexed to only one lithium ion.[34] So far we do not know if the lithium ion is coordinated to four or five acceptor atoms. The observed distances between the lithium ion and the oxygen of the carbonyl groups (Li–O between 210 and 225 pm) are in agreement with known X-ray data from lithium peptide complexes.[27d,e]

For the IRMA calculations, a correlation time of 1.5 ns was used instead of the 2.7 ns obtained from the $^{13}$C $T_1$ relaxation times. The former is an averaged value from different diagonal peak/cross-peak ratios of one NOESY spectrum in comparison to theoretical intensity matrixes created for different correlation times. For this approach, only NOEs involving backbone atoms were used to avoid the problem of the greater flexibility of side chains. In addition, the cross peaks in a NOESY spectrum at 300 MHz and 300 K support the shorter correlation time.

The 12 IRMA cycles in combination with the MD simulations lead to the following result: a $\beta$II'-turn-like structure is observed between residues 7 and 10, whereas no other secondary structure elements were found. No transannular hydrogen bond is observed; only one hydrogen bond is populated by more than 10%, between MeBmt$^1OH$ and Abu$^2NH$ (~100%). For comparison and to judge the effect of starting structure, the refinement procedure was carried out for two other structures: the conformations of CsA in $CDCl_3^{12d}$ (B) and CsA·CyP$^{22c}$ (C) are shown in Figure 7. The rms deviations of the backbone for the starting structures are A/B 2.7, A/C 2.3, and B/C 2.7 (where A indicates the random starting structure).

The starting structure B contains a cis peptide bond between residues 9 and 10. This was changed to all-trans after the first IRMA cycle. The root-mean-square (rms) deviations of the backbone atoms after three cycles of IRMA are A/B 1.6, A/C 2.7, and B/C 2.3. After a minimum $R$ factor[67] was obtained, 24 additional NOEs were introduced and two more IRMA cycles run. Ambiguities in the assignment of NOEs could be removed by comparison with the structure after three cycles of IRMA. At first the energy increases, because of the introduction of more distance restraints. After a minimum $R$ factor was again reached, another 23 distances were added, leading to a total of 130 constraints (including scaling peaks). This time the energy did not raise after the introduction of the new NOEs, indicating that the new distances fit within the structures. No convergence was achieved with these three structures (rms deviation of the backbone atoms: A/B 1.3, A/C 2.0, B/C 2.1). For this reason the distance restraints were set more restrictive; instead of the standard deviation from IRMA, obtained by averaging of the relaxation rates for the different mixing times, the averaged distances ±10% (for two cycles) and ±5% (for three cycles) were used.

There was still no convergence of the structures after these 12 IRMA cycles (rms deviation of the backbone: A/B 1.3, A/C 1.4, B/C 1.6). However, upon closer inspection, portions of the molecule are very similar. The large difference between A and B can be attributed to residues 3–6: the rms deviation of the backbone of amino acids 7–11 and 1–2 is 0.6 (for residues 7–10, 0.3). A hydrogen bond between Val$^5NH$ and Abu$^2CO$ is observed for B and not for A and C. The dihedral angles of residues 3 and 4 indicate in this region a $\beta$II' turn. For A and C a large deviation of the backbone is found for residues 3 and 4.

In spite of the lack of convergence, IRMA proved to be an extremely useful method: beginning from different starting

(63) Wiberg, K. B. *J. Am. Chem. Soc.* **1965**, *87*, 1070–1078.

(64) (a) Fletcher, R.; Reeves, C. M. *Comput. J.* **1964**, *7*, 149–154. (b) Williams, J. E.; Stang, P. J.; Schleyer, P. v. R. *Annu. Rev. Phys. Chem.* **1968**, *19*, 531–558.

(65) Koning, T. M. G.; Boelens, R.; Kaptein, R. *J. Magn. Reson.* **1990**, *90*, 111–123.

(66) (a) Kessler, H.; Kerssebaum, R.; Klein, A. G.; Obermeier, R.; Will, M. *Liebigs Ann. Chem.* **1989**, 269–294. (b) Ikura, M.; Kay, L. E.; Krinks, M.; Bax, A. *Biochemistry* **1991**, *30*, 5498–5504.

(67) Gonzalez, C.; Rullmann, J. A. C.; Bonvin, A. M. J. J.; Boelens, R.; Kaptein, R. *J. Magn. Reson.* **1991**, *91*, 659–664.
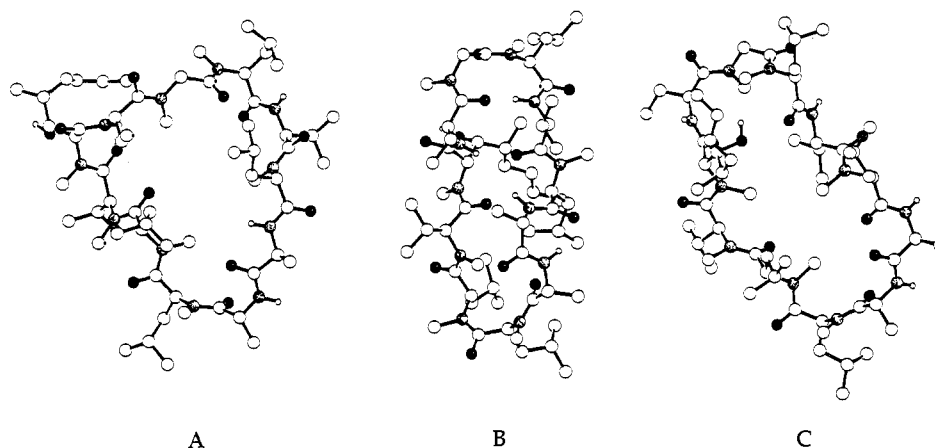
**Figure 7.** Different starting structures of CsA used for the calculations: (A) manual built, (B) CsA in $CDCl_3$, and (C) CsA bound to CyP. The MeLeu[4] residue is always in the upper right corner. The oxygen atoms are filled and the nitrogen atoms are stippled. Only the polar protons are shown.

**Table VI.** Backbone Dihedral Angles of the Lithium-Complexed CsA Compared to CsA·CyP and CsA[a]

| residue | Li·CsA $\phi$ | Li·CsA $\psi$ | CsA·CyP[b] $\phi$ | CsA·CyP[b] $\psi$ | X-ray CsA[c] $\phi$ | X-ray CsA[c] $\psi$ | CsA[d] $\phi$ | CsA[d] $\psi$ |
|---|---|---|---|---|---|---|---|---|
| MeBmt[1] | −153 | −79 | −125 | −167 | −84 | 123 | −89 | 112 |
| Abu[2] | 168 | −50 | −131 | 99 | −120 | 89 | −97 | 100 |
| Sar[3] | −63 (42) | 130 (−125) | 138 | −41 | 73 | −129 | 79 | −108 |
| MeLeu[4] | 95 (−125) | −138 (76) | −150 | 92 | −99 | 21 | −122 | 30 |
| Val[5] | −38 (−93) | 113 (109) | −75 | 136 | −112 | 126 | −104 | 123 |
| MeLeu[6] | −113 (−100) | −85 (66) | −114 | −159 | −90 | 99 | −82 | 88 |
| Ala[7] | −96 | 128 | −80 | 172 | −82 | 52 | −67 | 54 |
| D-Ala[8] | 76 | −118 | 83 | −156 | 87 | −124 | 80 | −137 |
| MeLeu[9] | −119 | 87 | −126 | 86 | −119 | 99 | −125 | 116 |
| MeLeu[10] | −110 | 128 | −117 | 153 | −138 | 64 | −131 | 86 |
| MeVal[11] | −111 | 70 | −131 | 80 | −102 | 125 | −120 | 133 |

[a] Dihedral angles are given in degrees. The values in parentheses denote the structure from calculation B. [b] Data taken from ref 19b. [c] Data taken from ref 9c. [d] Data taken from ref 9d.

structures, the distance restraints converged, shown in Figure 8 (right) for A and B. In comparison, the distances after the first IRMA cycle are shown in Figure 8 (left). A similar result was obtained for the distance restraints of C.

To investigate the lack of convergence, several additional simulation procedures under different conditions were carried out, for example, high-temperature dynamics for a longer time or incremental increase of the force constant $k_{dr}$ during the dynamics. For all these calculations, the distance restraints of A obtained after 12 IRMA cycles were used. To our surprise the peptide bond between residues Abu[2] and Sar[3] for C and between MeLeu[9] and MeLeu[10] for B adopted a cis configuration after several MD simulations. However, the NMR data are only consistent with the all-trans configuration and therefore dihedral restraining was used for the high-temperature MD runs.

Interesting results were obtained for a MD run for an extended period at high temperature and dihedral restraining; with the starting structures of B and C identical final structures were obtained (rms of the backbone 0.05). This structure is also identical to the structure of B after 12 IRMA cycles; e.g., the hydrogen bond between residues 2 and 5 is present. For A a different structure was found with deviations between residues 3 and 6 (rms of the backbone A/B 1.1 and A/C 1.2). To our surprise this structure was not identical to the structure of A obtained after 12 IRMA cycles. Repeating the MD simulation for A without dihedral restraining the same structure as after 12 cycles of IRMA is obtained (rms of the backbone 0.05). The structures of A with and without dihedral restraining differ only in the dihedral angles of residues 3 and 4. Again, different structures were obtained using the same set of distance restraints and the same starting structures, differing only in the performance of the MD run. This is a clear indication that the number of restraints is not sufficient in the region between residues 3 and 6. NOESY cross peaks of interest in this part of the molecule are Val[5]N$H$/MeLeu[4]C$_\alpha H$, Val[5]N$H$/Sar[3]C$_\alpha H$, MeLeu[4]N$Me$/
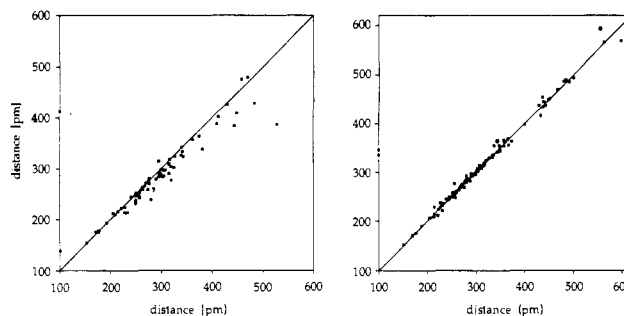


**Figure 8.** Comparison of the distances derived from IRMA for the starting structures A and B: distances after the first IRMA run (left); distances after 12 IRMA runs (right).

Abu[2]C$_\alpha H$, and Sar[3]N$Me$/Abu[2]C$_\alpha H$. The distances yield no clear distinction between the structures.

Now the question remains as to whether the structures can be distinguished by other experimental data. Two coupling constants are available: $^3J_{5NH/5C_\alpha H}$ (9.9 Hz) and $^2J_{3C_\alpha H/3C_\alpha H'}$ (17.1 Hz). A N$H$–C$_\alpha H$ coupling constant larger than 8.0 Hz suggests a $\phi$ of −80° to −160°.[68] The coupling constant fits with the dihedral angle $\phi$(Val[5]) = −93° of B, but not the value, −38°, observed for A. The dihedral angle for $\psi$ of Sar[3] obtained from the $^2J_{HH}$ coupling constant (10° or 170°)[69] is in disagreement with both A (130°) and B (−125°). The carbon relaxation times may indicate that MeLeu[4]CO is orientated into the ring, which is only found in A. There is no clear distinction between both structures; therefore, the energies were used as an additional criterion. The potential energy of B is smaller than for A ($\Delta E$ 35 kJ·mol⁻¹), which

(68) Kline, A. D.; Braun, W.; Wüthrich, K. *J. Mol. Biol.* **1988**, *204*, 675–694.

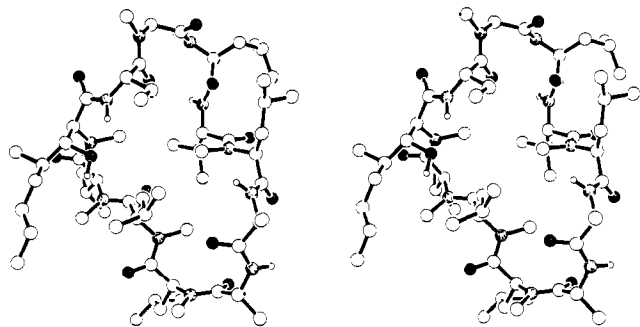(69) Bystrov, V. F. *Prog. Nucl. Magn. Reson. Spectrosc.* **1976**, *10*, 41–81.

*Novel Backbone Conformation of Cyclosporin A*

*J. Am. Chem. Soc., Vol. 114, No. 7, 1992* 2685



**Figure 9.** Stereoview of the mean structure of the lithium-complexed CsA in THF-$d_8$. This conformation was obtained after 12 IRMA cycles from averaging over 60 ps and restrained energy minimization. The oxygen atoms are filled and the nitrogen atoms are stippled. Only the polar protons are shown.

is obviously caused by the internal hydrogen bond in B. But the distance restraint energy considering all of the NOEs is smaller for A ($\Delta E$ 31 kJ·mol$^{-1}$). The structure of A is shown in Figure 9. In the tables, all of the dihedral angles are given for A. The backbone dihedral angles that are different between residues 3 and 6 for A and B are given in Table VI for comparison.

A $\beta$-turn-like structure was found in all conformations between residues 7 and 10 and was comparable to a convenient $\beta$II' turn with the D-amino acid in the $i + 1$ position as expected. The hydrogen bond of this turn between the residues $i$ (Ala$^7$) and $i + 3$ (MeLeu$^{10}$) is absent; the distance between Ala$^7$CO and MeLeu$^{10}$N*Me* is ~320 pm. However, the dihedral angles found for this $\beta$II' turn ($i + 1$, $\phi = 76°$, $\psi = -118°$, $i + 2$, $\phi = -119°$, $\psi = 87°$) are in agreement with the standard values. The large deviation of $\psi$ in position $i + 2$ has been found for CsA and its derivatives.[12c,20] It has been found in a 300-ps free molecular dynamics run that this new $\beta$II' turn is quite stable: only the positions of the atoms in this turn are retained as in the conformation with distance restraints. Calculations without restraints are usually useful to check the stability of a determined structure. However, in our case, the free simulations cannot be used to check the stability, since the calculations were performed without the metal ion and the restraints are necessary to mimic the ion and the solvent surrounding. In spite of this, the calculation shows the stability of the $\beta$ turn between residues 7 and 10. Even though the conformations of Li·CsA in comparison to CsA·CyP and CsA are different, the $\phi$ dihedral angles of residues 6–11 of Li·CsA and CsA·CyP are nearly identical. In addition, the $\psi$ of residues 7–11 are similar. The backbone dihedral angles of Li·CsA in comparison to CsA·CyP and CsA are given in Table VI.

The side-chain dihedral angles of Li·CsA are in good agreement with the obtained coupling constants, without fixing the side chains during the MD simulations. The preferred rotamer ($P_I$) of MeLeu$^6$ and MeLeu$^{10}$ is fulfilled in the structure with $-66°$ and $-64°$, respectively. Also Val and MeVal adopt the $\chi_1 = -60°$ conformation as derived from the coupling constants and MD as found for CsA in CDCl$_3$. In the CyP complex, both valines adopt the $P_{II}$ rotamer ($\chi_1 = 180°$). It is often found that MD simulations in vacuo without a fixing of the side chains to their preferred conformation lead to physically unrealistic pictures due to vacuum effects. In this case however the preferred rotamers were obtained without fixing of the $\chi_1$ dihedral angles, indicating that there are enough NOE constraints to determine the proper rotamer. Obviously the system is determined quite well locally due to the high number of intraresidual NOEs. The side-chain dihedral angles of Li·CsA in comparison to CsA·CyP and CsA are given in Table VII. The rms fluctuations of the torsions during the trajectories are also given in this table to illustrate internal flexibilities during these trajectories.

The total number of 130 restraints looks very impressive for such a small molecule. However, there are only six long-range restraints which normally are important in determining the structure. Obviously the lithium ions force the molecule to adopt an open, extended structure, similar to that found for metallo-

**Table VII.** Side-Chain Dihedral Angles of Li·CsA Compared to the Values of CsA Bound to CyP and CsA Derived from the Structure in CDCl$_3$ and the Crystal Structure[a]

| residue | | Li·CsA | CsA·CyP[b] | X-ray CsA[c] | CsA[d] |
|---|---|---|---|---|---|
| MeBmt$^1$ | $\chi_1$ | −76.1 (6.7) | −24 | −166 | −77 (2.8) |
| | $\chi_2$ | 179.7 (7.8) | 171 | 74 | 91 (2.7) |
| | $\chi_3$ | −153.4 (19.0) | 54 | −179 | −180 (3.8) |
| | $\chi_4$ | 15.9 (173.1) | −122 | −126 | 168 (17.1) |
| | $\chi_5$ | −179.5 (8.5) | 178 | −175 | −180 (2.3) |
| Abu$^2$ | $\chi_1$ | −76.8 (17.7) | −78 | −178 | −70 (4.2) |
| MeLeu$^4$ | $\chi_1$ | −137.8 (18.3) | −67 | −51 | −151 (13.3) |
| | $\chi_2$ | 59.4 (10.4) | −99 | −54 | −172 (4.6) |
| Val$^5$ | $\chi_1$ | −62.7 (7.6) | 179 | −51 | −61 (2.5) |
| MeLeu$^6$ | $\chi_1$ | −66.4 (8.8) | −49 | −176 | −178 (2.3) |
| | $\chi_2$ | −71.5 (9.8) | 175 | −177 | −175 (2.7) |
| MeLeu$^9$ | $\chi_1$ | −140.7 (41.5) | −55 | −54 | −60 (2.6) |
| | $\chi_2$ | −140.6 (40.9) | 170 | −63 | −70 (3.7) |
| MeLeu$^{10}$ | $\chi_1$ | −63.7 (8.0) | −74 | −163 | −148 (9.5) |
| | $\chi_2$ | −68.8 (10.0) | 155 | −169 | −78 (6.3) |
| MeVal$^{11}$ | $\chi_1$ | −55.5 (8.4) | −175 | −53 | −60 (2.4) |

[a] The dihedral angles are given in degrees. The values in parentheses denote the rms fluctuatioin obtained by averaging. [b] Data taken from the averaged structure of ref 19c. [c] Data taken from ref 9c. [d] Data taken from ref 9d.

thionenin,[70] where the cadmium ions in the complex also lead to a lack of long-range effects and a less defined structure. As mentioned above, no transannular hydrogen bond was found for Li·CsA beginning with the random starting structure. In all trajectories after 12 IRMA cycles, the hydrogen bond between MeBmt$^1$O*H* and Abu$^2$N*H* is populated ~100%, whereas in CsA in CDCl$_3$, the MeBmt$^1$O*H* forms a hydrogen bond with its own carbonyl group.

## Conclusion

The conformation of CsA in THF-$d_8$ is similar to the one in CDCl$_3$, whereas the addition of LiCl to CsA in THF-$d_8$ produces a drastic change in conformation. In the complex the peptide bond between residues 9 and 10 is trans, similar in this regard to the conformation of CsA bound to its receptor cyclophilin. The $\beta$-stranded sheet within the $\beta$II' turn and the three transannular hydrogen bonds observed in free CsA in solution and in the crystal are lost upon complexation with lithium. No transannular hydrogen bond is observed in the conformation of the complex, although a new $\beta$II'-turn-like structure is observed between residues 7 and 10 without a "real" hydrogen bond (CO−*Me*N) between residues $i$ and $i + 3$. This turn is observed in all calculations with the different starting structures, indicating that this part of the molecule is well determined. Starting from different conformations, the refinement procedure leads to convergence of the seven residues 7–11 and 1–2, whereas the region between residues 3–6 is not sufficiently determined because of the lack of long-range NOEs. The structure in the backbone between residues 7 and 11 observed here is similar to that recently reported for CsA bound to cyclophilin. Obviously complexation by lithium ions drastically changes the backbone conformation. We assume that the orientation of carbonyl oxygens to the metal induces the largest effect on the backbone. However, the breaking of the intramolecular hydrogen bond may also influence the backbone conformation, including cis/trans isomerism. It is of special interest that the addition of LiCl to CsA in THF leads to a drastic increase of the PPIase inhibition, showing the importance of the trans peptide bond between residues 9 and 10. We conclude that new derivatives of CsA must contain a trans peptide bond between residues 9 and 10.

## Experimental Section

**NMR Measurements.** All NMR spectra were recorded on Bruker spectrometers (AM250, AM300, AM500, AMX500, and AMX 600).

(70) Frey, M. H.; Wagner, G.; Vasak, M.; Sørensen, O. W.; Neuhaus, D.; Wörtgötter, E.; Kägi, J. H. R.; Ernst, R. R. *J. Am. Chem. Soc.* **1985**, *107*, 6847–6851.

Two samples of CsA in THF-$d_8$ (99.5% $^2$H atoms; Aldrich) containing 20 mg/0.4 mL (42 mmol/L) and 186 mg/0.65 mL (238 mmol/L) were prepared in 5-mm tubes. For Li·CsA, one sample containing 18.6 mg of CsA in 0.6 mL of THF-$d_8$ (26 mmol/L) and 20.3 mg of LiCl (30.9 equiv) in a 5-mm tube was prepared. All samples were degassed by five freeze–pump–thaw cycles. All chemical shifts are referenced to the downfield THF-$d_8$ signal at 3.58 ppm for $^1$H and 67.4 ppm for $^{13}$C. Unless indicated, all experiments were measured at 300 K. For the uncomplexed CsA in THF-$d_8$, we have measured 1D $^1$H and $^{13}$C spectra, temperature gradients (between 300 and 330 K), DQF-COSY at 300 and 250 K, TOCSY, NOESY at 300 and 250 K, ROESY, HMQC, TOC-SY-DEPT,[71] and COLOC.[72] For the latter two experiments, the highly concentrated sample was used because of the low sensitivity of X-detected experiments. Since the results from these experiments are not further utilized in this publication, no parmeters are explicitly given. All 2D spectra were recorded with quadrature detection in both dimensions; TPPI[73] was used in $F_1$. The spectra were processed on a Bruker Aspect X32 computer. All information about sizes and data points of the spectra are given in real points. All proton-detected heteronuclear experiments except the HMBC were run using a BIRD$_x$ pulse [90°$_x$($^1$H)–$D_2$–180°$_x$($^1$H), 180°$_x$($^{13}$C)–$D_2$–90°$_{-x}$($^1$H)][74] in the preparation period of the pulse sequence for presaturation of the protons bound to $^{12}$C. This method allows rapid pulsing and is higher in sensitivity.[75] The recovery delay $D_4$, occurring in these experiments, covers the time between the end of the BIRD$_x$ pulse and the beginning of the pulse sequence. In the following, the parameters of all experiments of Li·CsA are given:

**(1) 1D $^1$H NMR spectra:** Size 16K, sweep width 5555.56 Hz, pulse length 9.0 $\mu$s (ca. 82° pulse), relaxation delay 2.0 s, 64 acquisitions. The spectra for determination of the temperature gradients were recorded between 300 and 330 K in steps of 10°. Size 16K, sweep width 5555.53 Hz, pulse length 8.0 $\mu$s (ca. 82° pulse), relaxation delay 2.0 s, 128 acquisitions.

**(2) 1D $^{13}$C NMR spectrum [AMX500]:** size 32K, sweep width 26 315.79 Hz, pulse length 6.0 $\mu$s (ca. 60° pulse), relaxation delay 2.5 s, 16 000 acquisitions.

**(3) 1D $^{13}$C $T_1$ Relaxation times [AMX500]:** sequence $D_1$–180°–$D_4$–90°–$t_1$, proton decoupling. Size 32K, sweep width 26 315.79 Hz, relaxation delay 10 s, delay times $D_4$ = 50, 100, 150, 200, 250, 300, 400, 500, 750, 1000, and 1500 ms, 90° pulse 9.6 $\mu$s, 4096 acquisitions.

**(4) DQF-COSY spectrum [AM500]:** sequence $D_1$–90°–$t_1$–90°–$D_2$–90°–$t_2$. Relaxation delay $D_1$ = 1.5 s, delay $D_2$ = 2 $\mu$s; 90° pulse 7.7 $\mu$s, acquisition time 307.2 ms, sweep width in $F_1$ and $F_2$ 5681.82 Hz, size 2K, 64 acquisitions, 540 increments.

**(5) TOCSY spectrum [AM300]:** sequence $D_1$–90°–$t_1$–MLEV17–$t_2$. Relaxation delay $D_1$ = 1.5 s, mixing time for MLEV-17 (10.4 kHz) 60.0 ms, 90° pulse 24.0 $\mu$s, acquisition time 368.6 ms, sweep width in $F_1$ and $F_2$ 3311.26 Hz, size 2K, 48 acquisitions, 540 increments.

**(6) NOESY spectra [AMX600]:** sequence $D_1$–90°–$t_1$–90°–$\tau_{mix}$–90°–$t_2$. Relaxation delay $D_1$ = 2.8 s, mixing times $\tau_{mix}$ = 40, 80, 120, 160, and 200 ms, 90° pulse 10.7 $\mu$s, acquisition time 282.6 ms, sweep width in $F_1$ and $F_2$ 7246.38 Hz, size 2K, 32 acquisitions, 512 increments.

**(7) ROESY spectrum [AM300]:** sequence $D_1$–90°–$t_1$–90°–spinlock–90°–$t_2$. Relaxation delay $D_1$ = 1.5 s, mixing time for spinlock (4 kHz) 150 ms, 90° pulse 10.3 $\mu$s, ROESY pulse 1.5 $\mu$s (flip angle 13°), ac-

quisition time 368.6 ms, sweep width in $F_1$ and $F_2$ 3311.26 Hz, size 2K, 40 acquisitions, 550 increments.

**(8) E. COSY spectrum [AMX500]:** sequence $D_1$–90°–$t_1$–90°–$D_2$–90°–$t_2$. Relaxation delay $D$ = 1.2 s, delay $D_2$ = 3 $\mu$s, 90° pulse 10.9 $\mu$s, acquisition time 1.483 s, sweep width in $F_1$ and $F_2$ 2762.43 Hz, size 4K, 36 acquisitions, 1024 increments.

**(9) $^1$H,$^{13}$C-HMBC spectrum [AM500]:** sequence $D_1$–90°($^1$H)–$D_2$–90°($^{13}$C)–$D_4$–90°($^{13}$C)–$t_1$/2-180°($^1$H)–$t_1$/2-90°($^{13}$C)–$t_2$($^1$H). Relaxation delay $D_1$ = 1.3 (1.5) s, $D_2$ = 60 ms, 90° pulse 10.8 $\mu$s ($^1$H), 12.7 (13.0) $\mu$s ($^{13}$C), acquisition time 368.6 ms, sweep width in $F_1$ 15 000 Hz and in $F_2$ 5555.56 Hz, size 2K, 256 acquisitions, 128 increments. The spectrum was recorded and processed phase sensitive, followed by a magnitude calculation in $F_2$.

**(10) $^1$H,$^{13}$C-HMQC spectrum [AMX500]:** sequence $D_1$–BIRD–$D_4$–90°($^1$H)–$D_2$–90°($^{13}$C)–$t_1$/2-180°($^1$H)–$t_1$/2-90°($^{13}$C)–$D_2$–$t_2$($^1$H), GARP[76] decoupling. Relaxation delay $D_1$ = 138.0 s, $D_2$ = 3.57 ms, $D_4$ = 172.0 ms, 90° pulse 10.9 $\mu$s ($^1$H), 12.0 $\mu$s ($^{13}$C), acquisition time 184.3 ms, sweep width in $F_1$ 18 796.99 Hz and in $F_2$ 5555.56 Hz, size 1K, 96 acquisitions, 247 increments.

**(11) $^1$H,$^{13}$C-DEPT-HMQC with TOCSY transfer spectrum [AMX500]:** sequence $D_1$–BIRD–$D_4$–90°($^1$H)–$D_2$–90°($^{13}$C),180°($^1$H)–$D_2$–$\beta$($^1$H),180°($^{13}$C)–$D_2$–$t_1$/2-180°($^1$H)–$t_1$/2-90°($^{13}$C)–$D_2$–$t_2$($^1$H), GARP decoupling. Relaxation delay $D_1$ = 138.0 ms, $D_2$ = 3.57 ms, $D_4$ = 172.0 ms, mixing time for MLEV-17 (10.4 kHz) 57.0 ms, 90° pulse 5.8 $\mu$s ($^1$H), 10.4 $\mu$s ($^{13}$C), $\beta$ 11.6 $\mu$s (with a 180° DEPT pulse; correlations to methylene carbon atoms appear 180° out of phase compared to the remaining multiplicities), acquisition time 184.3 ms, sweep width in $F_1$ 18 796.99 Hz and in $F_2$ 5555.56 Hz, since 1K, 240 acquisitions, 400 increments.

**(12) $^1$H,$^{13}$C-HQQC spectrum [AMX500]:** sequence $D_1$–BIRD–$D_4$–90°($^1$H)–$D_2$–180°($^1$H),90°($^{13}$C)–$D_2$–90°($^1$H)–$t_1$/2-180°($^1$H)–$t_1$/2-90°($^1$H),180°($^{13}$C)–$D_2$–180°($^1$H),90°($^{13}$C)–$D_2$–$t_2$($^1$H), GARP decoupling. Relaxation delay $D_1$ = 138.0 s, $D_2$ = 3.57 ms, $D_4$ = 172.0 ms, 90° pulse 10.9 $\mu$s ($^1$H), 12.0 $\mu$s ($^{13}$C), acquisition time 184.3 ms, sweep width in $F_1$ 4201.68 Hz and in $F_2$ 5555.56 Hz, size 1K, 48 acquisitions, 128 increments.

(71) Kessler, H.; Gemmecker, G.; Köck, M.; Osowski, R.; Schmieder, P. *Magn. Reson. Chem.* **1990**, *28*, 62–67.

(72) Kessler, H.; Griesinger, C.; Zarbock, J.; Loosli, H.-R. *J. Magn. Reson.* **1984**, *57*, 331–336.

(73) Marion, D.; Wüthrich, K. *Biochem. Biophys. Res. Commun.* **1983**, *113*, 967–974.

(74) Garbow, J. R.; Weitekamp, D. P.; Pines, A. *Chem. Phys. Lett.* **1982**, *93*, 504–509.

(75) Bax, A.; Subramanian, S. *J. Magn. Reson.* **1986**, *67*, 565–569.

(76) Shaka, A.; Barker, P. B.; Freeman, R. *J. Magn. Reson.* **1985**, *64*, 547–552.